Shelf basin exchange along the Siberian continental margin: modification of Atlantic Water and Lower Halocline Water

Dorothea Bauch, Ekaterina Cherniavskaia, Leonid Timokhov

PII: S0967-0637(16)30014-0
DOI: http://dx.doi.org/10.1016/j.dsr.2016.06.008
Reference: DSRI2651

To appear in: *Deep-Sea Research Part I*

Received date: 15 January 2016
Revised date: 24 May 2016
Accepted date: 22 June 2016

Cite this article as: Dorothea Bauch, Ekaterina Cherniavskaia and Leoni Timokhov, Shelf basin exchange along the Siberian continental margin modification of Atlantic Water and Lower Halocline Water, *Deep-Sea Researc Part I,* http://dx.doi.org/10.1016/j.dsr.2016.06.008

Shelf basin exchange along the Siberian continental margin: modification of Atlantic Water and Lower Halocline Water

Dorothea Bauch[1*], Ekaterina Cherniavskaia[1,2], Leonid Timokhov[2]

[1]GEOMAR Helmholtz Centre for Ocean Research Kiel, Wischhofstr. 1-3, 24148 Kiel, Germany
[2]Arctic and Antarctic Research Institute, 38 Bering str., St. Petersburg 199397, Russia

Manuscript for Deep Sea Research I
[*]Corresponding authors: Dorothea Bauch; dbauch@geomar.de

Abstract:

Salinity and stable oxygen isotope ($\delta^{18}O$) evidence shows a modification of Atlantic Water in the Arctic Ocean by a mixture of sea-ice meltwater and meteoric waters along the Barents Sea continental margin. On average no further influence of meteoric waters is detectable within the core of the Atlantic Water east of the Kara Sea as indicated by constant $\delta^{18}O$, while salinity further decreases along the Siberian continental slope.

Lower halocline waters (LHW) may be divided into different types by Principal Component Analysis. All LHW types show the addition of river water and an influence of sea-ice formation to a varying extent. The geographical distribution of LHW types suggest that the high salinity type of LHW forms in the Barents and Kara seas, while other LHW types are formed either in the northwestern Laptev Sea or from southeastern Kara Sea waters that enter the northwestern Laptev Sea through Vilkitsky Strait. No further modification of LHW is seen in the eastern Laptev Sea but the distribution of LHW-types suggest a bifurcation of LHW at this location, possibly with one branch continuing along the continental margin and a second branch along the Lomonosov Ridge. We see no pronounced distinction between onshore and offshore LHW types, as the LHW components that are found within the halocline over the basin also show a narrow bottom-bound distribution at the continental slope that is consistent with a shelf boundary current as well as a jet of water entering the western Laptev Sea from the Kara Sea through Vilkitsky Strait.

List of abbreviations:

Water masses:

LHW	Lower halocline water

AW	Atlantic Water
modAW	modified Atlantic Water
BSBW	Barents Sea Branch Water
FSBW	Fram Strait Branch Water

Currents:

WSC	West Spitzbergen Current
EGC	East Greenland Current
ASBB	Arctic Shelf Break Branch
VSC	Vilkitsky Strait Current

Geographical names:

SZ	Severnaya Zemlya
VS	Vilkitsky Strait
BS	Barents Sea
KS	Kara Sea
LS	Laptev Sea
ESS	East Siberian Sea

Others:

AO	Arctic Ocean oscillation
PCA	Principal Component Analysis
EOF	Empirical Orthogonal Functions

Keywords: Arctic Ocean; Siberian shelves; shelf basin exchange; stable oxygen isotopes; water masses; Principal Component Analysis; Arctic Halocline; Lower Halocline Water; Atlantic Water; Arctic Circumpolar Boundary Current

1. Introduction

Due to strong stratification the Arctic Ocean halocline insulates the sea-ice cover from the underlying Atlantic Water (AW) heat and thus plays a fundamental climatological role (e.g. Rudels et al. 1996). With the ongoing climate change in the Arctic Ocean involving alterations in sea-ice patterns (e.g. Overland and Wang, 2013; Timokhov et al., 2012) and increasing meteoric freshwater input (Zhang et al., 2013) significant changes are to be expected for the upper Arctic Ocean and halocline (e.g. Itkin et al., 2015 Bauch et al., 2010; Holland and Bitz 2003; Bekryaev et al., 2010). Hence, further knowledge is needed on the current structure, formation processes and regions of the Arctic Ocean halocline.

In the Eurasian part of the Arctic Ocean the Lower Halocline is formed by modification of AW over the Barents and Kara seas (Rudels, 2004; Steele and Boyd, 1998; Aagaard et al., 1981); it has salinities of about ~33 to 34.5 and temperatures close to the freezing point of sea-water. However, temperatures may be slightly higher at the continental margin of the Laptev Sea (LS). This could be attributed to an enhanced vertical exchange above the

continental shelf slope (Dmitrenko et al., 2011), although the underlying mechanism is under debate (Timokhov et al, 2015).

Here we study the shelf-basin exchange along the Siberian continental margin. The influx of large quantities of river water and low salinity shelf waters occurs at the eastern LS continental margin and has been investigated before (Bauch et al 2014). In this study we will focus on the layers below about 50m water depth down to the depth of the Atlantic core and specifically ask: are Lower Halocline Water (LHW) and AW modified by shelf waters along the continental slope of the Kara and Laptev shelves? As sea-ice processes are a dominant feature on the shelves, an application of $\delta^{18}O$ analysis and salinity/$\delta^{18}O$ mass balances are highly appropriate tools that enable us to identify and quantify the signal of sea-ice modification (melting and sea-ice formation) within the water column (e.g. Östlund and Hut, 1984; Bauch et al., 1995). Such shelf-basin interactions may have strong interannual and regional variability and are expected to be relatively small within the subsurface water masses such as the LHW and AW. First, we evaluate the properties of the core of AW in the Eurasian Basin of the Arctic Ocean in respect to geographical and inter annual variability. As the contributions of shelf components are expected to be small, this requires a high measurement precision of the $\delta^{18}O$ data. Therefore average $\delta^{18}O$ values are considered for the evaluation of the AW where variations are in the same range as the measurement precision. Then, we use a Principal Component Analysis (PCA) of the upper 50-250m of the water column including $\delta^{18}O$ derived parameters and also hydrochemical data to investigate the influence of shelf waters in LHW and the modification of LHW along the Siberian continental margin. The approach of a PCA is chosen to decrease the degrees of freedom within this diverse multi-parameter oceanographic data set that includes strong gradients combined with strong inter annual variations.

2. Methods:

Samples for $\delta^{18}O$ analyses at the Eurasian continental margin were collected in summer from 2005 to 2009 within the framework of the Nansen and Amundsen Basins Observational System (NABOS) program (expedition technical reports are available at http://nabos.iarc.uaf.edu/cruise/reports.php) and Polarstern expedition ARKXXII/2 in summer 2007 (see expedition reports in Schauer, 2008) (Fig. 1). Also shown are $\delta^{18}O$ data from Polarstern expeditions in 1993 and 1995 (Frank, 1996). In all cases water samples were taken with a conductivity-temperature-depth (CTD)-rosette with an accuracy of at least ±0.002 S/m in conductivity and ±0.005°C in temperature.

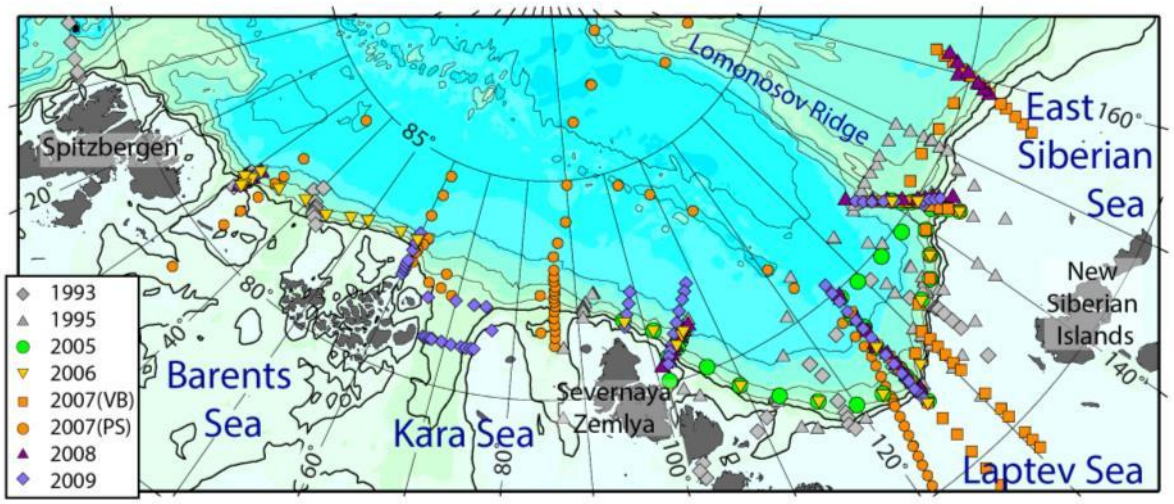

Fig. 1: Station distribution of NABOS data 2005-2009 and Polarstern data 1993, 1995 and 2007.

Accuracy for all presented $\delta^{18}O$ is at least ±0.04‰ (Bauch et al., 2010, 2011a+b, 2013). All $H_2{}^{18}O/H_2{}^{16}O$ ratios were calibrated with Vienna Standard Mean Ocean Water (VSMOW) and reported in the usual δ-notation (Craig, 1961). A subset of the NABOS stable isotope data from the LS continental margin were published before (Bauch et al., 2011a, 2011b). Data taken in 2007 were published without special attention on LHW (Bauch et al., 2011b).

Based on $S/\delta^{18}O$ mass balance calculations fractions of AW, meteoric water and sea-ice meltwater are derived following Bauch et al. (1995; 2011a). It is assumed that each sample is a mixture between fractions of Atlantic derived water (f_{mar}), river runoff (f_r), and sea-ice meltwater (f_{SIM}). As only stations west of 150°E are discussed, no additional analysis for the influence of Pacific derived waters is necessary (Abrahamsen et al., 2009; Bauch et al., 2011b). The mass balance is governed by the following equations:

$$f_{mar} + f_r + f_{SIM} = 1,$$

$$f_{mar} * S_{mar} + f_r * S_r + f_{SIM} * S_{SIM} = S_{meas},$$

$$f_{mar} * O_{mar} + f_r * O_r + f_{SIM} * O_{SIM} = O_{meas},$$

where f_{mar}, f_r, and f_{SIM} are the fractions of marine water, river runoff, and sea-ice meltwater (SIM) in a water parcel, and S_{mar}, S_r, S_{SIM}, O_{mar}, O_r and O_{SIM} are the corresponding salinities and $\delta^{18}O$ values of the endmembers (Tab. 1). S_{meas} and O_{meas} are the measured salinity and $\delta^{18}O$ of the water samples. Technically f_r refers to meteoric water, which includes local precipitation, but as river runoff dominates in the study area we refer to river runoff for simplicity. For the freshwater endmembers a $\delta^{18}O$ of -20‰ is chosen for river water and for sea-ice -2‰ $\delta^{18}O$ and 4 salinity; for further details on the selection of end-members refer to Bauch et al. (2010; 2011b). For the analysis of the Arctic halocline the properties of the

Atlantic core in the south-western Nansen Basin (e.g. Bauch et al., 1995; 34.92 salinity and 0.3‰ $\delta^{18}O$) are taken as the marine endmember. For the analysis of the Atlantic layer within the Arctic Ocean the marine endmember needs to refer to a water mass outside of the Arctic Ocean. Therefore, for the analysis of the Atlantic layer, we take as a marine endmember the properties of the Atlantic core in the West Spitsbergen Current (WSC; 35.05 salinity and 0.303‰ $\delta^{18}O$ with standard deviations of ±0.05 and ±0.014‰, respectively. Data from 1993 and with 8 stations at ~79°N and 2-9°E).

Tab. 1: End-Member Values Used in Mass Balance calculations[a]

End-Member	Salinity	$\delta^{18}O$ (‰)
River water (f_r)	0	-20(1)
Sea-ice meltwater (f_{SIM})	4(1)	-2(1)
Marine water (f_{mar})		
for halocline analysis	34.92(5)	0.30(5)
for Atl. layer analysis	35.05(1)	0.30(1)

[a]Numbers in parentheses are the estimated uncertainties within the last digit in our knowledge of each end-member value.

All fractions are net values reconstructed from the $\delta^{18}O$ and salinity signatures of each sample, and reflect the time-integrated effects on the sample volume over the residence time of the water in the Arctic Ocean. Negative SIM fractions (f_{SIM}) reflect the amount of water removed by sea-ice formation and are proportional to the addition of brines to the water column. SIM fractions may be negative during summer season sampling if the winter sea-ice formation signal exceeds the summer melt signal. Based on a measurement precision of 0.04‰, in $\delta^{18}O$ the error in calculated fractions is about 0.2% for both sea-ice meltwater and river water fractions. An additional systematic error or shift depends on the exact choice of end-member values. When end-member values are varied within the estimated uncertainties (Tab. 1), both fractions are shifted by up to ~1%, but results are always qualitatively preserved even when tested with extreme end-member variations (see Bauch et al., 2011b). For the comparison of values and to detect differences only the propagated error of measurement precision needs to be considered as comparison of fractions are only made with the same set of endmembers. Potential inter annual variability of endmembers is not critical as the mean residence time of shelf waters is 3.5±2 years (Schlosser et al., 1994) and thus halocline water formation takes several years.

Principal Components (PCs) and Empirical Orthogonal Functions (EOFs) were calculated using function PRINCOMP of the MATLAB software package. The data set consisted of temperature (T), salinity (S), f_{SIM}, fr, silicate (Si), phosphate (P) and nitrate (N) data taken

between 2005 and 2009 at ~30°E, 60°E, 100°E, 126°E, ~145°E and ~160°E. At these positions cross slope sections were covered in most years or at the least in more than one year. We included f_{SIM}, fr, instead of $\delta^{18}O$ as calculated fractions already incorporate the discrepancy relative to salinity measurements and are much easier to directly interpret.The results when including $\delta^{18}O$ instead of f_{SIM}, fr differ only marginally. For an analysis of LHW and modified Atlantic Waters (modAW) located above the Atlantic core we calculated PCs for samples between 50 and 250m depth. The upper 50m of the water column were omitted from the PCA to avoid strong signals from relatively local surface variability. Data from 1993 and 1995 were not included in the PCA as sample coverage within the upper 250m is relatively sparse. Data were organized as a matrix in which the columns are T, S, f_{SIM}, fr, Si, P, N, and the rows are the samples, i.e. 627 values, for all 140 available stations. The T, S, f_{SIM}, fr, Si, P and N data were normalized using the data means and standard deviations in order to avoid influence of different scales of input data. EOF decomposition was made for normalized data and EOFs as well as PCs were obtained. North's "rule of thumb" was applied to estimate reliability of obtained EOFs (North et al., 1982). According to this test, the first three EOFs are statistically significant as the distances between them is larger than the sampling errors. The first three EOFs describe over 85% of total data variance within our dataset. Each EOF is a combination of values T, S, f_{SIM}, fr, Si, P and N, and the PCs are a combination of variations of T, S, f_{SIM}, fr, Si, P and N in principal component space.

Cluster analysis was performed on the first three PCs following Ward (1963). The measure of the distance between the nodes was introduced through the Euclidean metric. The points with minimal linkage distance were combined into groups (clusters), where T, S, f_{SIM}, fr, Si, P or N values has minimal difference. Analysis of linkage distance in a dendrogram shows that it is expedient to distinguish no more than 8 clusters (Fig. 2) as differences in linkage distance are rapidly decreasing below the chosen threshold. Points that were placed in the same cluster by Ward's method are usually also located close to each other in the PC1 versus PC2 scatter plot (Fig. 3). An exception is cluster c5 that is mostly defined by deviations seen in PC3 and only appeared in the 2009 dataset.

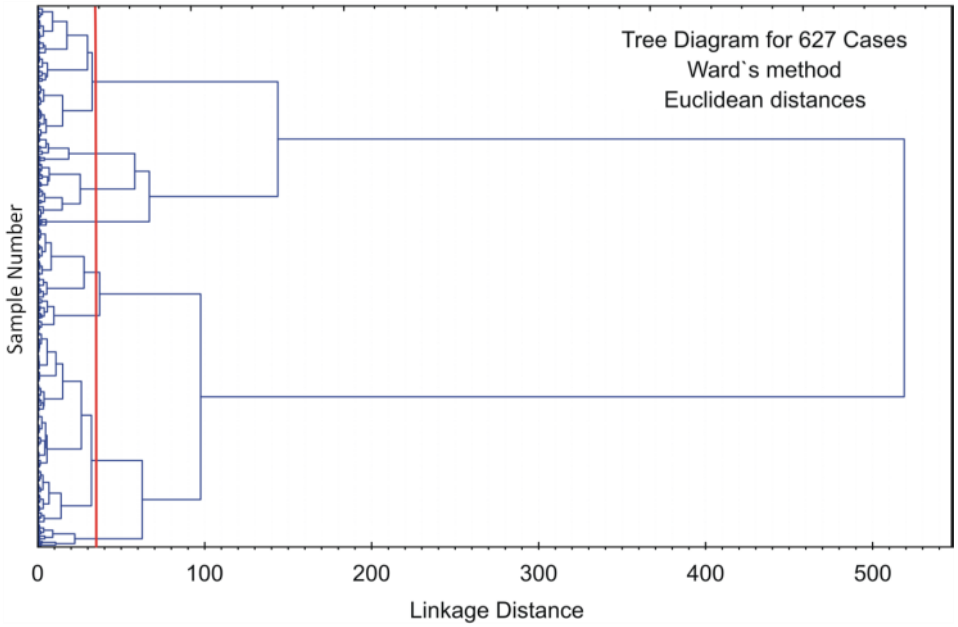

Fig. 2: Dendrogram of Euclidian distances for the analysed data following Ward (1963). The red line indicates the chosen threshold that determines the number of clusters.

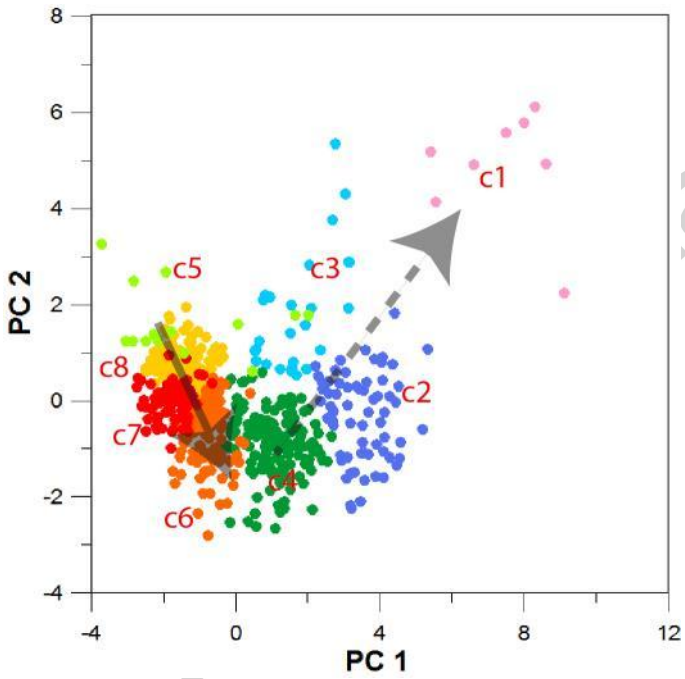

Fig. 3: Scatter plot of main principal components PC1 and PC2. PCA clusters can be assigned to water masses: AW (yellow c8; red c7), mod AW (orange c6; lightgreen c5) and LHW (green c4; turquoise c3; blue c2; pink c1). The pattern in PCA clusters can be assigned to water mass modifications. The solid arrow indicates a modification of AW to modAW involving sea-ice meltwater processes and the stippled arrow indicates a modification of modAW to LHW types connected to sea-ice related brine contributions.

3. Results

As the $\delta^{18}O$ values of meteoric waters is very low in the Arctic region $\delta^{18}O$ is at first order linearly correlated to salinity for all stations along the Siberian continental shelf (Fig. 4). Due

to sea-ice processes station data may deviate to lower or higher salinities compared to the direct mixing line between the average $\delta^{18}O$/salinity values of Arctic river water and the signature of the inflowing AW. Melting of sea-ice lowers the salinity of the underlying water column as sea-ice is relatively fresh with an estimated average salinity of ~4. The formation of sea-ice on the other hand extracts water from the surface layer and adds brines to the water column that are released rapidly from the crystal structure of the ice through brine channels. Thus sea-ice processes impact salinity, while the $\delta^{18}O$ signature of the water is changed by a fractionation factor that is small compared to the $\delta^{18}O$ signal of meteoric water. For a detailed analysis of the $\delta^{18}O$/salinity signature of the dataset (Fig. 4) it is necessary to carefully distinguish by region and depth levels or water mass.

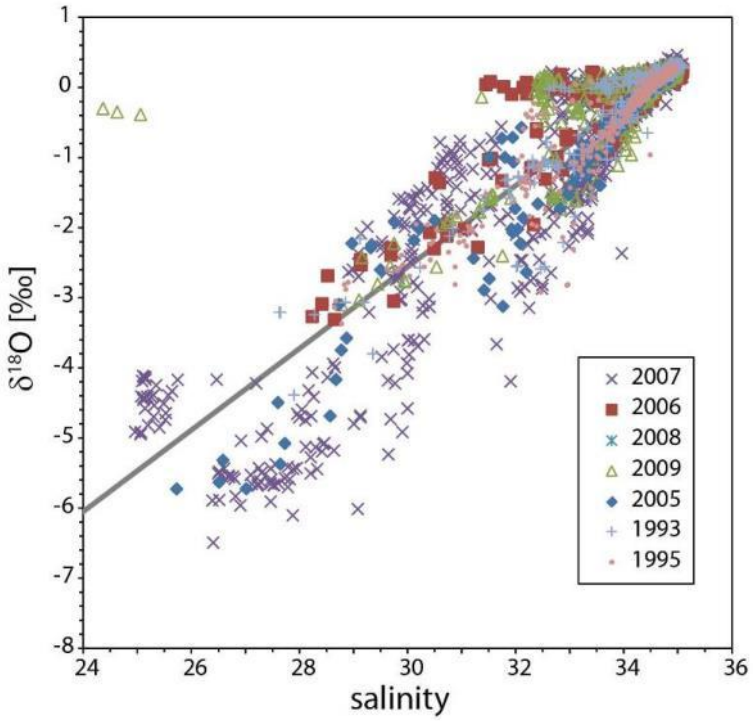

Fig. 4: Salinity versus $\delta^{18}O$ from the upper 500m of the water column along the Siberian continental slope. The direct mixing line between AW (34.92 salinity and 0.3‰ $\delta^{18}O$) and river water endmembers (-20‰ $\delta^{18}O$) is shown in gray for orientation.

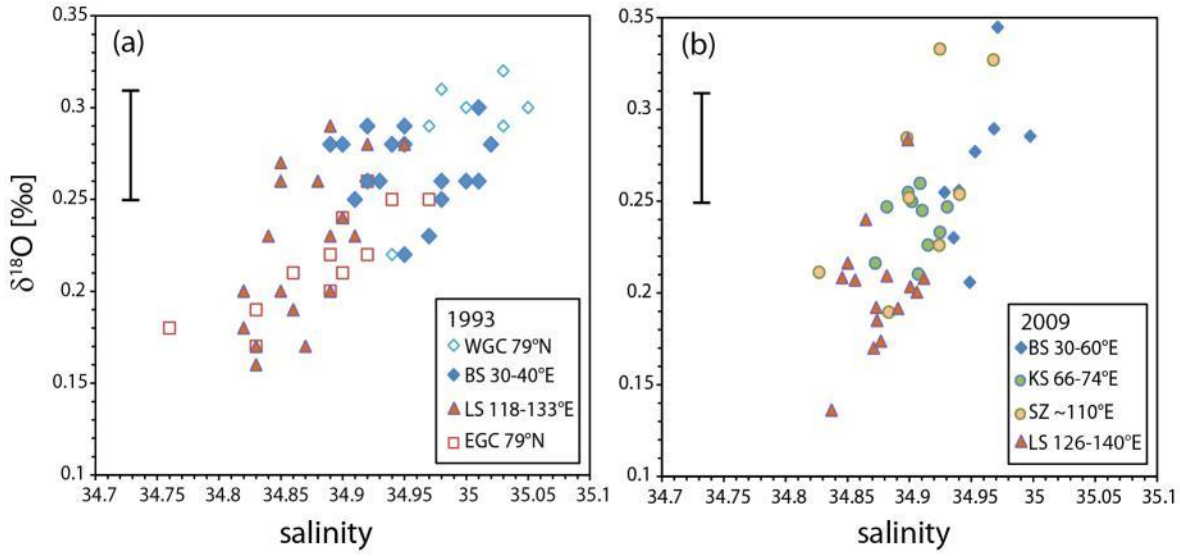

Fig. 5: Atlantic Water $\delta^{18}O$ and S taken within the temperature maximum for years with wide geographical coverage (a) 1993 and (b) 2009. Sampling areas are indicated for the West Spitzbergen Current (WSC), East Greenland Current (EGC) and at the continental slope north of the Barents Sea (BS), Kara sea (KS), Severnaya Zemlya (SZ), Laptev Sea (LS). Error bars are shown for each dataset (for both 1993 and 2009 the errors are ±0.03).

Tab. 2: Averages of $\delta^{18}O$ and S within the temperature maximum of the Atlantic core in the West Spitzbergen Current (WSC) and at the continental slopes of the Barents Sea (BS), Kara Sea (KS), Severnaya Zemlya (SZ), Laptev Sea (LS), East Siberian Sea (ESS) and in the East Greenland Current (EGC). Data are combined for all years (2005-2009 NABOS and PS 1993 and 1995). Given are also the standard deviation (σ) and the number of data points (n). Linear correlation with R^2=0.93 is $\delta^{18}O$=0.32 S -11(±3) for data between the WSC and 128°E.

area	Salinity	σ	$\delta^{18}O$[‰]	σ	n
WSC at 79°N	35.03	0.05	0.30	0.01	15
BS 30-40°E	34.98	0.05	0.26	0.05	28
BS 40-65°E	34.92	0.06	0.21	0.06	34
KS 65-90°E	34.90	0.05	0.20	0.07	36
SZ 90-110°E	34.89	0.06	0.21	0.09	38
LS 110-128°E	34.88	0.03	0.21	0.05	67
LS 128-150°E	34.86	0.03	0.22	0.04	79
ESS 150-165°E	34.84	0.02	0.22	0.04	19
EGC at 79°N	34.88	0.05	0.22	0.03	6

The Atlantic layer is easily identified by temperatures above 0°C and may be represented by the properties at the Atlantic core temperature maximum usually located between about 200-350m depth. All $\delta^{18}O$ and S data taken in the Atlantic core display a systematic linear

relationship with a correlated eastward decrease in $\delta^{18}O$ and salinity (Tab. 2; Fig. 5). At the shelf break of the Barents Sea (BS) an average decrease of ~0.1‰ in $\delta^{18}O$ and ~0.1 in salinity relative to AW properties in the WSC is seen. Eastwards and thus downstream from the BS average salinity decreases along the LS and East Siberian Sea (ESS) slope (by a total of at least ~0.08; see Tab. 2), while $\delta^{18}O$ values show no significant change in averaged data (see Tab. 2). Only in individual data sets from single years a decrease in salinity as well as $\delta^{18}O$ is also seen between BS and LS (Fig. 5). Inter annual comparison of single profiles e.g. north of Severnaya Zemlya (SZ) within Fram Strait Branch Water (FSBW) shows that 2006 station data has lower $\delta^{18}O$ values relative to its salinity within the salinity range of the Atlantic core compared to all other years (Fig. 6).

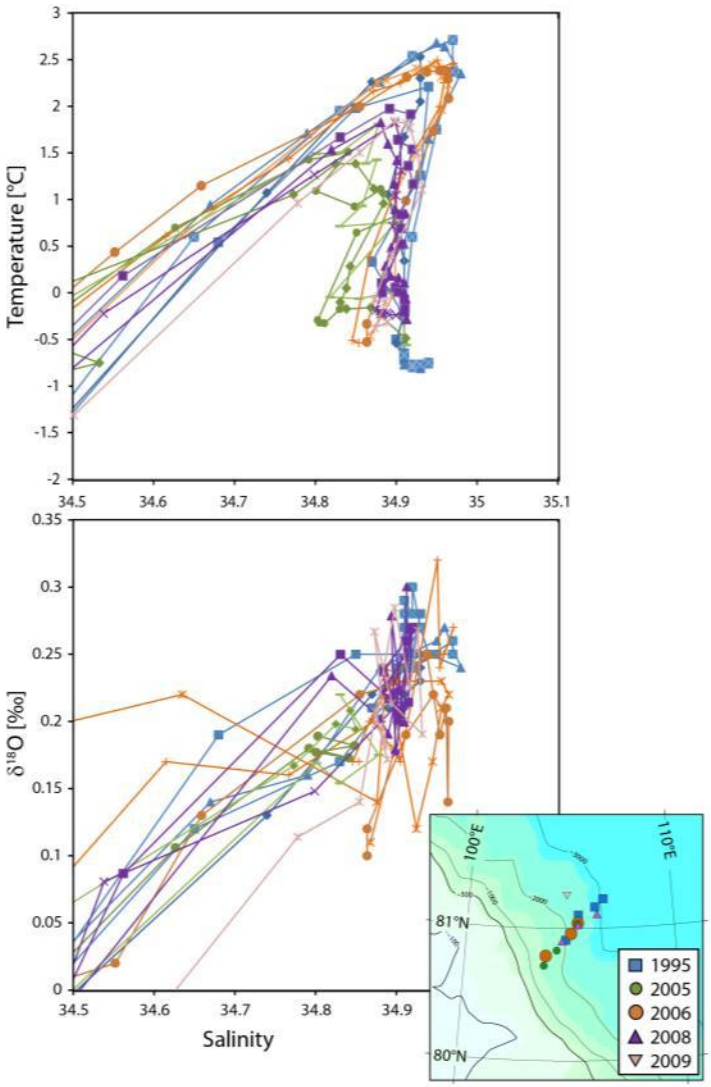

Fig. 6: Comparison of single profiles taken near SZ within FSBW in 1995 (blue), 2005 (green), 2006 (orange), 2008 (violet) and 2009 (pink).

Tab. 3: Averages properties of T, S and $\delta^{18}O$ within the temperature maximum of the Atlantic core (values between 200-300m with T in the range of ±0.1° to T_{max}) north of SZ (~105°E). Fractions of river water fr and sea-ice meltwater f_{SIM} are calculated relative to 35 salinity and 0.30‰ $\delta^{18}O$ for the Atlantic inflow and -20‰ $\delta^{18}O$ for river water. Also given are the standard deviations (grey numbers) and the number of samples n.

year	T[°C]		S		$\delta^{18}O$[‰]		f_{SIM} [%]		fr[%]		n
1995	2.31	0.40	34.93	0.04	0.25	0.01	0.11	0.10	0.26	0.07	12
2005	1.34	0.31	34.82	0.03	0.18	0.02	0.05	0.13	0.60	0.09	10
2006	2.29	0.15	34.94	0.03	0.22	0.05	-0.12	0.26	0.43	0.23	19
2008	1.51	0.30	34.89	0.04	0.21	0.03	0.03	0.18	0.44	0.15	17
2009	1.70	0.18	34.91	0.01	0.26	0.03	0.19	0.19	0.22	0.15	3

For analysis of LHW and modAW located above the Atlantic core we applied a PCA to station data (T, S, Si; P, N, f_{SIM} and f_r) from the upper 50 to 250m of the water column. We distinguished 8 clusters (c1-c8) based on the first three PCs. PC1 reflects 56% of the data variability and appears to be mainly associated with salinity (Tab. 4 and Fig. 3). PC2 and PC3 reflect 19% and 10% of data variability, respectively. The first two PCs therefore reflect ~75% of the variance and may be taken as representative for the data variability. By their temperature and salinity signature (e.g. Rudels et al. 1996) clusters 1- 4 can be assigned to LHW, which occupy an average depths of ~45-110m, clusters 5 and 6 at ~ 150 m water depth can be attributed to modAW. And AW are represented by clusters 7 and 8 (see Tab. 4 and Fig. 3).

4. Discussion

4.1 Alteration of Atlantic Water

AW flow northwards in the WSC and enter the Arctic Ocean through Fram Strait in the FSBW or across the Barents and Kara seas in the Barents Sea Branch Water (BSBW) (e.g. Schauer et al., 2002). The correlated decrease in $\delta^{18}O$ and S in the properties of the Atlantic core relative to the WSC occurs along the continental slope of the BS and therefore within the FSBW (Fig. 5, Tab. 2). This decrease in $\delta^{18}O$ and S must be from isotopically light meteoric waters originating either from direct precipitation or river runoff. Ice that forms in areas with high fractions of river water is a mixture of sea-ice and freshwater-ice. Therefore river water may also be transported in frozen form as freshwater-ice e.g. in the BS where small river water contribution coincide with high sea-ice meltwater fraction (Bauch et al., 2011a). In all these cases surface processes involving meteoric fresh waters must have been involved in the modification of the Atlantic core. As the travel time within the Arctic Circumpolar Boundary Current may be in the order of several years (Woodgate et al., 2001; Mauldin et al., 2010)

synoptically sampled data from different regions may reflect inter annual differences in AW inflow. This may explain why a decrease in $\delta^{18}O$ between the BS and the LS is seen in individual datasets from 1993 and 2009 (Fig. 5), while this signal is lost when all years are averaged (Tab. 2). Downstream from the BS $\delta^{18}O$ values within the Atlantic core show on average no further alteration but there is a decrease of at least ~ 0.08-0.14 in salinity between the BS and the ESS continental slope (Tab. 2). FSBW and BSBW interact and mix along the continental slope of the Kara Sea (KS) and a mixture of both continues east along the continental slope of the LS (Schauer et al., 2002). Our data indicates that on average the mixture of FSBW and BSBW does not involve further addition of meteoric water within the AW core. Bottom waters from the Kara or the Laptev shelves contain considerable fractions of river water in combination with a signal from sea-ice formation (Bauch et al., 2003; Bauch et al. 2005). Therefore it may be assumed that on average also no significant entrainment of shelf waters into BSBW and FSBW waters occurs downstream from the BS. The observed decrease of salinity within the Atlantic core must be due to other processes that do not involve meteoric waters or shelf waters due to missing $\delta^{18}O$ decrease. Also no significant alteration in S as well as in $\delta^{18}O$ is seen between the LS and the EGC.

Inter-annual changes in AW properties may occur due to changes within the inflow of FSBW and BSBW or due to inter-annual variability in AW modification along the Siberian continental slope. Therefore an inter-annual comparison needs to be done regionally. Stations at similar positions north of SZ reveal inter annual differences in Atlantic layer properties between 1995, 2005, 2006, 2008 and 2009 (Fig. 6). Only 2006 data deviate from the direct mixing line between pure river and pure marine waters with lower $\delta^{18}O$ at relatively high salinity. In all other years $\delta^{18}O/S$ values within the Atlantic core fall on the direct mixing line. Therefore relatively low salinities in 2005, intermediate salinities in 2008 and 2009 as well as high salinities in 1995 all point to an upstream variation in AW properties that involve meteoric waters. Such modifications may occur regionally within the freshwater balance of the inflowing AW, within the FSBW or in the BSBW. The $\delta^{18}O/S$ deviations from the direct mixing line in 2006 on the other hand indicate a more local modification with addition of brine-enriched waters released into the water column during sea-ice formation. The addition of negative sea-ice meltwater contributions (brine) to the Atlantic layer near SZ in 2006 is on average -0.3% and varies within the range of -0.6 and 0% and thus strongly compared to all other years without brine contributions (see Fig. 6 and Tab. 3). This indicates a rather variable contribution of brine-enriched waters to AW at salinities of ~34.86 -34.96 near SZ in 2006.

Such a variable contribution of brine waters to the Atlantic core is detected also further to the east in 2006 with an average contribution of 0.12% of sea-ice related brine to the Atlantic layer (all data between SZ and ~145°E). While this contribution of sea-ice derived brine is small and variations are within the error of 0.20% for a single measurement, variations are significant when averaged and standard errors of the mean are considered. In all other years the values of brine-enriched waters in the Atlantic core are variable within the measurement precision only and indicate no significant contribution of brine relative to the Atlantic inflow. Therefore our data indicate that not only near SZ an enhanced amount of sea-ice related brine is present within the Atlantic core but all along the Siberian continental margin between SZ and 145°E in 2006. As this brine signal within the Atlantic layer was absent the previous summer, the question remains whether this intrusion of brines was formed synoptically all along the Siberian continental slope in winter 2005/2006 or whether it was possibly transported to these positions from a single event further upstream? Cascading of water masses from polynya activity may occur directly north of SZ (Ivanov and Golovin, 2007) and thus lead to the addition of sea-ice related brine within the Atlantic layer. Further eastwards, at our sampling positions at ~126°, 133° and 145°E, surface waters are too fresh to speculate on local production of high salinity waters from polynya activity. An average annual mean velocity of about 3-5cm/s was measured within the Atlantic layer north of the central LS slope (Woodgate et al., 2001). Adopting this mean velocity, a transport of AW from SZ to ~145°E could occur within 7-12 months. Therefore AW modified by sea-ice formation e.g. in the northern KS region or north of SZ in October 2005 could have been sampled at ~126°, 133° and 145°E in September 2006. It is important to note that temperature and salinity properties of AW north of SZ in summer 2006 are somewhat different than properties sampled at eastern positions in other years. Therefore we conclude that it is likely that AW with a brine component sampled at 126°E, 133°E and 145°E in summer 2006 might have been formed near SZ e.g. in early winter 2005 and was transported along the shelf break. The core of AW sampled at SZ in summer 2006 with higher salinities may have been modified during a later event. In accordance with this speculation, BSBW in 2006 was found to have a longer residence time over the BS shelf that may have led to a high brine contribution relative to earlier years (Dmitrenko et al., 2009). While in the BS melting of sea-ice is known to be dominant, sea-ice formation nevertheless also plays a role in the formation of BSBW (Dmitrenko et al., 2009).

4.2 Origin of different LHW types

As the first three PCs reflect ~85% of the data variance the derived clusters may be assumed to be representative of the data variability contained in the original T, S, f_{SIM}, fr, Si, P and N data and each cluster is identified with a water type. All types of LHW (c1-4) have a brine contribution (Tab. 4). Brine and river contributions are coupled and therefore the LHW component with highest salinity (c4) has not only the smallest river but also the smallest sea-ice related brine contribution. The coupling between sea-ice related brine and river water contributions is typical for shelf waters, indicating sea-ice formation in coastal polynyas where river water is present (Bauch et al., 2011b). LHW type c4 is the only LHW type that is found at SZ and westwards (Fig. 7, 8).

Tab. 4: Average properties of clusters. Listed are the parameters included in the PCA and in addition the average depth and the average $\delta^{18}O$ value of each cluster. Also given are the standard deviations (grey numbers).

c#		T		S		Si		P		N		f_{SIM}		fr		depth		$\delta^{18}O$	
1	LHW	-1.6	0.1	33.0	0.4	10.7	2.1	0.7	0.1	6.4	2.0	-3.6	0.9	8.6	1.4	48	8	-1.46	0.27
2		-1.5	0.3	34.0	0.2	4.5	1.5	0.5	0.1	5.7	1.4	-1.5	0.6	4.0	0.8	63	18	-0.53	0.17
3		-1.0	0.3	34.2	0.2	8.2	2.1	0.7	0.0	8.8	1.1	-0.8	0.4	2.7	0.8	98	31	-0.27	0.17
4		-0.9	0.6	34.4	0.2	4.2	1.1	0.6	0.1	7.5	1.5	-0.4	0.4	1.8	0.6	110	43	-0.08	0.12
5	mod.AW	0.7	1.5	34.7	0.3	4.0	0.6	1.7	0.4	10.1	2.2	-0.5	0.5	1.2	1.3	148	72	0.06	0.27
6		0.8	0.9	34.7	0.1	4.1	0.9	0.6	0.2	9.8	1.5	-0.1	0.5	0.7	0.3	151	67	0.15	0.06
7	AW	1.7	1.0	34.8	0.1	4.4	0.5	0.8	0.1	11.4	0.9	0.0	0.3	0.3	0.3	169	59	0.24	0.06
8		2.0	0.7	34.9	0.1	5.2	0.8	0.8	0.1	11.5	1.3	-0.5	0.3	0.6	0.3	187	54	0.18	0.06

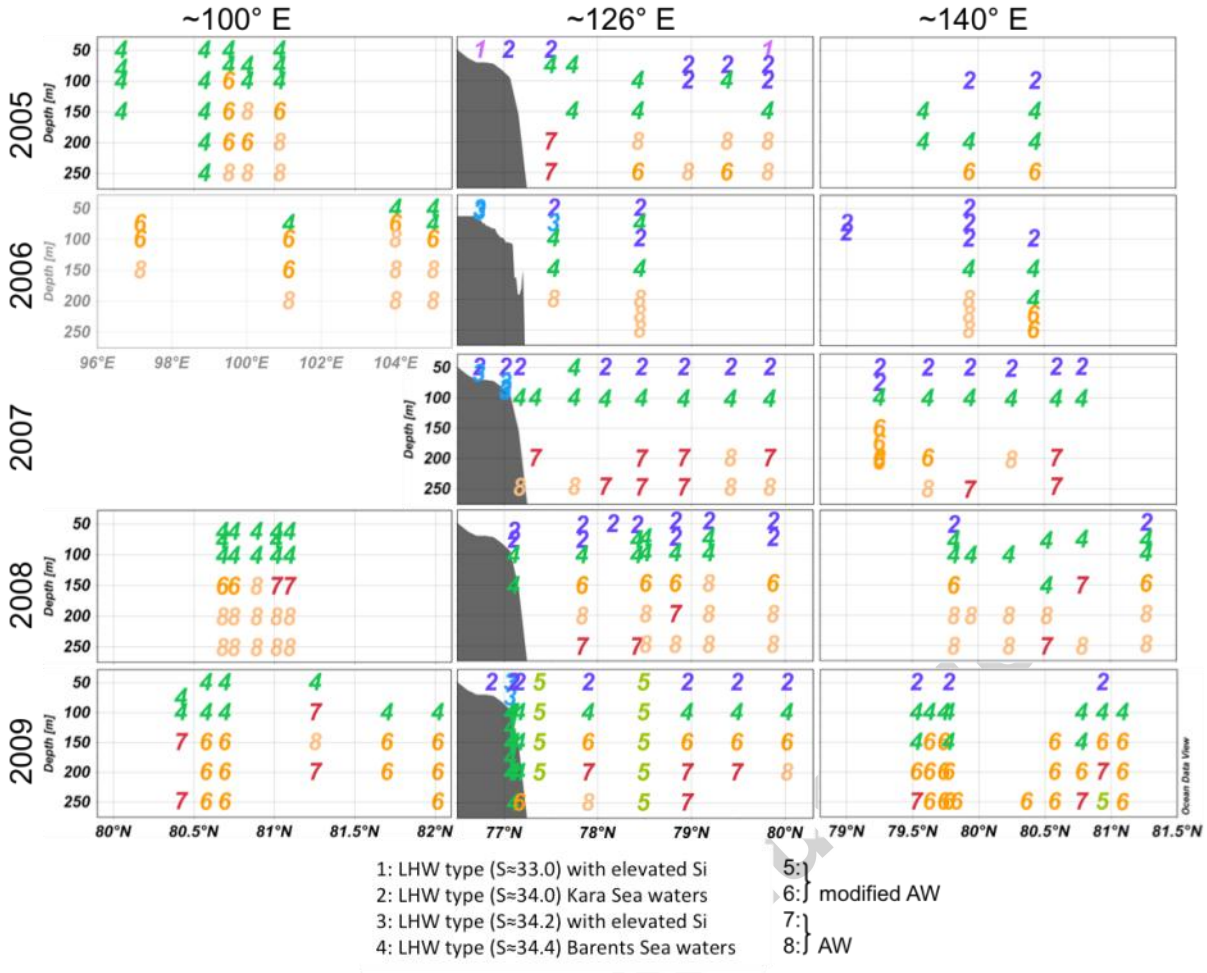

Fig. 7: Geographical distribution of clusters shown for cross slope sections north of SZ (left panels), at ~126°E (middle panel) and at ~140°E (right panels). Note that the 2006 section near SZ is parallel to the shelf break; all other sections are perpendicular to the shelf break.

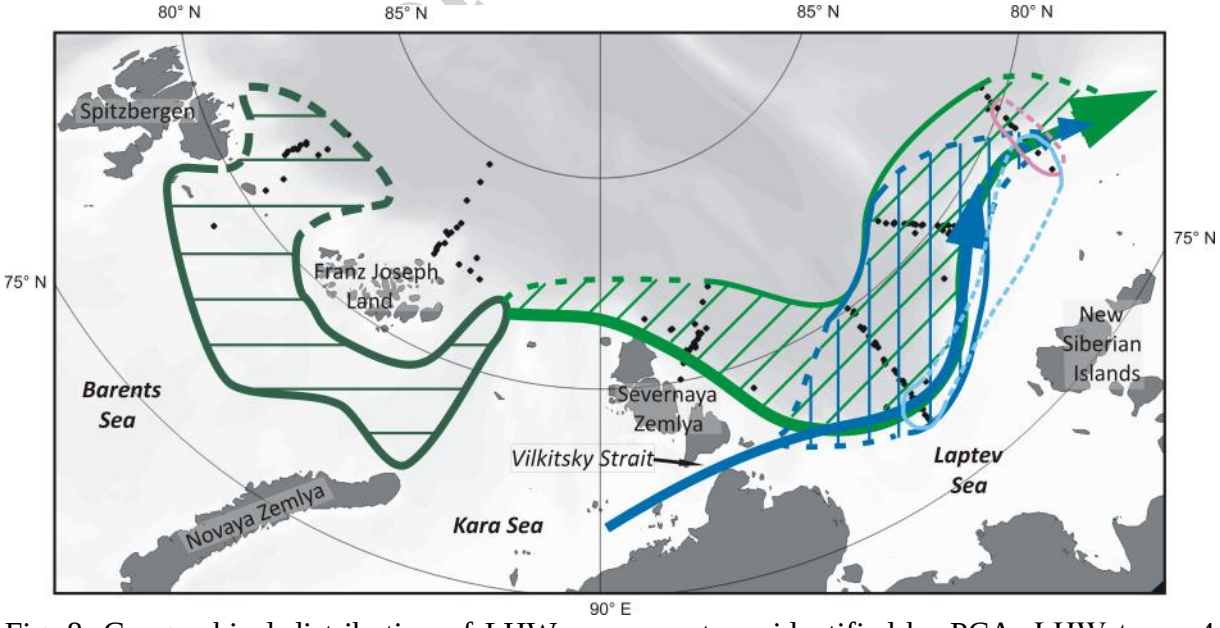

Fig. 8: Geographical distribution of LHW components as identified by PCA: LHW type c4 (green) and c2 (blue) are found over the basin as well as in bottom bound features along the

continental slope that are identified with the Arctic Shelf Break Branch (Aksenov et al., 2011) and the Vilkitsky Strait Current (Janout et al., 2015), respectively. The extent of the area for the formation of LHW component c4 (dark green) was taken from Aksenov et al. 2011. Also sketched are occurrence of LHW type c1 (pink) and c3 (light blue).

As the temperature of LHW type c4 is, at -0.87°C, still relatively high, this LHW type must be a mixture of a relatively warm water mass and a cold and brine enriched shelf water mass similar to modAW type c6 but with a larger shelf water component, e.g. from the southeastern Kara Sea region. A formation of LHW type c4 from modAW type c5 on the other hand is not possible as brine contributions in both clusters are similar, while the river component in c4 is higher (see arrows shown in Fig. 3). The broad appearance of LHW type c4 at the shelf break north of SZ, probably indicates that it leaves the KS toward the north through St. Anna and Voronin Trough (Fig. 8). Only a few samples show LHW type c4 also at the 30°E locations (not sampled all years). Our observation of a broad appearance of LHW type c4 at the shelf break north of SZ is consistent with a formation of LHW in the BS and KS region (Rudels et al., 1996; Aksenov et al., 2011) and its advection eastwards along the continental slope in a narrow boundary current, the Arctic Shelf Break Branch (ASBB) (Aksenov et al., 2011). We find evidence for such a narrow topographically-steered boundary current as LHW type c4 is found also at depth directly at the continental slope at 126°E in 2009 and near SZ in 2005 (Fig. 7). As the boundary current is described as extremely narrow (Aksenov et al., 2011), this feature was probably not captured in most other years due to wide spacing between bottle stations. Similar to the ASBB, an extremely narrow jet of AW near SZ was reported by Pnyshkov et al. (2015) from NABOS 2005 that was captured in a single CTD station only and that was missed by wider spacing of our bottle stations. From the geographical distribution and the vertical distribution at the continental slope (Fig. 7) we conclude that LHW type c4 can be identified with the water mass transported in the ASBB described by Aksenov et al. (2011). Based on this assumption our cluster analysis suggests that the same water mass that feeds the ASBB also feeds into the halocline layer at about 100 to 150m water depth off-slope where LHW type c4 is also found in all years (Fig. 7, 8).

LHW types c1, c2 and c3 have lower salinity and appear in contrast to LHW type c4 only east of SZ: c2, c3 are captured at 126°E and eastward, while c1 appears mostly north of the ESS at ~145°E and ~160°E. Therefore LHW types c2, c3 must either be formed directly in the north-western LS or enter the north-western LS through Vilkitsky Strait (VS) and are probably formed in the south-eastern KS. Shelf waters from the KS are described to leave the KS through VS in a narrow boundary current, the Vilkitsky Strait Current (VSC) (Janout et al., 2015). The VSC is found to be blocked under certain local atmospheric conditions, which

leads to storage of freshwater in the KS (e.g. in 2004) and release in the following year (e.g. in 2005). The VSC is modelled to overlay and merge with the ASBB directly north-east of VS at the continental slope (Janout et al., 2015). We hypothesize that LHW type c2 has its origin in the south-eastern KS and is the same water mass that is described to leave the KS in the VSC (Janout et al., 2015). Our arguments are (i) c2 contains locally-formed shelf water which can be seen in its characteristic f_{SIM}/fr ratio (Bauch et al, 2011), (ii) dense station coverage at the continental slope in 2009 shows c2 at 50-100m water depth and directly on top of c4 that forms the ASBB between 100 and 250m water depth at the continental slope (Fig. 7; see 126°E section in 2009), which is consistent with model results (Aksenov et al., 2011; Janout et al., 2015). While the VSC and the ASBB are very narrow currents, it appears that the water mass components that feed these currents are also transported into the basin (see Fig. 7, 8). The transport of these LHW components further off-slope may either occur directly or from recirculating waters in the eastern Eurasian Basin (Rutgers van der Loeff et al, 2012) that may be fed by waters from the boundary currents over a wider region.

The relative contribution of each LHW type to total LHW volume might be roughly estimated by evaluating the spatial distribution of each LHW type within our sampling array (Fig. 7). This approach does not account for dynamical features, e.g. likely enhanced transport of LHW types c4 and c2 in the ASBB and VSC, respectively. Nevertheless LHW types c2 and c4 within the 126°E section account for ~30 to 50% and ~50 to 70%, respectively, for 2005-2009. LHW c2 and c4 contribute at a ratio of roughly 1:1 in 2008 and 2009 and 1:2 in 2005 and 2007. LHW types c1 and c3 contribute less than 4% in all years.

Earlier analyses focused on the LS slope at 126°E suggest a separation in on-slope and off-slope components of LHW (Dmitrenko et al., 2011). Our PCA-derived LHW types do not support a general distinction in on-slope and off-slope components as the main LHW types c4 and c2 are found as part of the ASBB and VSC on-slope as well as over the basin further off-slope (Fig. 7). Only LHW types c3 and c1 are found largely on the continental slope at ~126 and ~160°E, respectively. LHW type c3 is relatively similar to c2 and c4 and differs mainly in silicate composition coupled amount of brine/river contribution. Dmitenko et al. discusses LHW at different depth range (~51 m) and salinity (33.70 to 33.96) and, thus LHW type c3 at ~ 98 m and 34.2±0.2 salinity is not likely responsible for previous assessments of LHW distinction in on-slope and off-slope components. Also these LHW types account for only ~4% of LHW along 126°E when dynamical features are ignored. While temperatures within the depth layer of LHW are slightly elevated at the shelf break of the continental margin

(Dmitrenko et al., 2011; Timokhov et al., 2015) the underlying mechanism responsible for the observed elevation in temperature remains unknown (Timokhov et al., 2015).

LHW types c1 and c3 both have elevated silicate values but are rather different in salinities (~33.0 and ~34.2). These clusters are observed in 3 out of 5 years and may only be formed sporadically. In addition these high Si types are found north of the central LS at ~126°E and north of the ESS at ~160°E, while both are missing at the intermediate position north of the New Siberian Islands at ~145°E where the main outflow of shelf water from the LS occurs (Bauch et al., 2014; 2011a; 2009). Due to extremely high Si values in LS bottom waters it is tempting to speculate on an admixture of small contributions of LS bottom waters to form LHW with elevated Si values. But the largely missing brine component in high Si waters north of the LS shows that shelf waters from the LS are not responsible for elevated Si concentrations in LHW type c3 (Bauch et al., 2014). The high silicate LHW found north of the LS shelf break may instead pick up elevated silicate values from bottom re-suspension directly at the shelf break (Bauch et al., 2014). However, our observations are mostly taken during late August and September when the area is most accessible by ship-based expeditions. As we are missing winter data from the central or northern LS there is further room for speculation on a high salinity shelf water mass that might contribute a brine and a silicate component to LHW.

Both modAW types have a small river water contribution accompanied by small brine contributions (c5, c6; see Tab. 4). ModAW type c5 is found only within the 2009 dataset and is characterized by high P values (Tab. 4). ModAW types are found close to the surface in the BS and northern KS region where they are probably formed in different regions or different seasons according to their river and brine contributions. Net sea-ice melting is known to occur in the BS (Dmitrenko et al., 2009) and a small river water contribution might also be present in this region either from local rivers or transported there by ice with a high meteoric water content (see Bauch et al., 2011a). The slight brine contributions in the modAW components that are formed in the BS are nevertheless consistent as the fractions for the LHW analysis are calculated relative to AW properties in the south-western Nansen Basin (see methods) instead of to AW properties in the WSC (compare e.g. Dmitrenko et al., 2009).

The distribution of AW types shows no discernable pattern and thus the separation of two AW types may have no physical meaning. The variations of AW properties are extremely small and in the applied analysis all regions and years are combined.

4.3 Interannual variations

Annually different station and depth distributions do not allow a detailed inter annual comparison e.g. into features such as the ASBB. Nevertheless it is quite apparent that the depth distribution of LHW types varies between years (Fig. 7). While LHW type c4 is found at about 150m water depth at all locations between SZ and 140°E e.g. in 2005 and 2006 (see Fig. 7), it is found at shallower depth e.g. in 2008 and 2009 (see Fig. 7; note that the 150m depth level was not sampled in 2007). A boundary depth of 150m was chosen to trace the variations of LHW depth and modAW thickness. CTD data was used to allow for a denser data and station coverage compared to bottle data. Only stations with bottom depth deeper than 1200m were included to avoid distortions from dynamical processes directly at the continental slope. Average waters properties at 150m reflect variations in depth distribution of c4 across this boundary depth. Average properties of waters at the boundary depth at ~126°E are lower in T_{150m} and S_{150m} when c4 is deeper in the water column in 2005 and 2006 and higher in T_{150m} and S_{150m} when c4 is shallower in the water column in 2008 and 2009 (Tab. 5).

Tab. 5: Average waters properties at 150m taken from CTD data for stations along 126°E. Also given are the standard errors.

Year	T_{150}		S_{150}	
2005	0.28	0.07	34.56	0.01
2006	0.44	0.26	34.65	0.02
2007	0.88	0.12	34.68	0.02
2008	1.07	0.11	34.67	0.01
2009	0.94	0.11	34.71	0.03

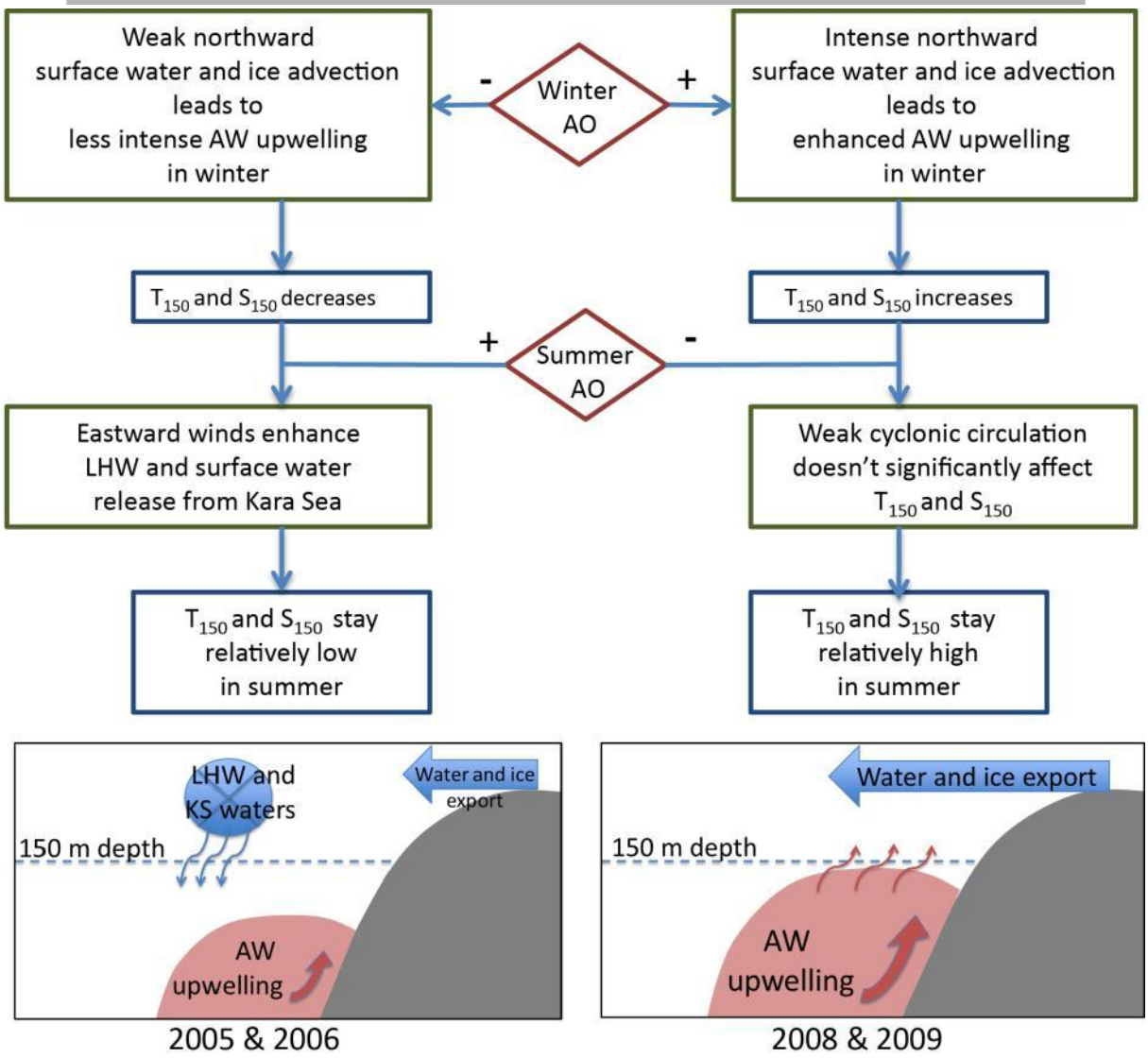

Figure 9: Sketch of proposed mechanisms and flow chart of vertical shifts in LHW in response to atmospheric forcing with winter AO- and summer AO+ in 2005 and 2006 (left panel) and winter AO+ and summer AO- in 2008 and 2009 (right panel).

For a further evaluation we look at the regional climate indices. The winter (October to March) atmospheric circulation indices AO are defined as the first EOF of the Sea Level Pressure (SLP) distribution between 20-90°N (e.g. Overland and Wang, 2010). For all years covered in this study the winter AO (October to March) was of opposite sign to the summer AO (July to September). We find positive correlation between both T_{150m} and S_{150m} and the winter AO and negative correlation with the summer AO. (Due to the limited time series high correlation coefficients are required for significance. Only the relation of T_{150m} and summer AO is significant with a Spearman correlation coefficient of -0.9). Such variations in halocline water depth and accordingly AW displacement have been noted before on a seasonal scale (Dmitrenko et al., 2006). But what is the underlying mechanism behind these variations in the boundary depth between LHW and AW within the water column? Dmitrenko et al. (2006)

described the mechanism of seasonal variability of the AW core at the LS continental slope that is shifted upwards and closer to the slope in winter when the large scale circulation supports off shore winds at the LS continental margin that induce slight upwelling of Atlantic Water. We hypothesize in agreement with Rigor et al. (2002) that under AO+ with strong cyclonic circulation there is a strong northward advection of surface waters and ice that might enhance AW upwelling compared to years with AO- when AW upwelling might be weaker (Fig. 9). Coherent with this concept we observe a shallow distribution of c4 and higher T_{150m} and S_{150m} with positive winter AO in summers 2008 and 2009 when modAW and AW are potentially still found at shallower depths within the water column even under negative summer AO. In 2005 and 2006 on the other hand a negative winter AO leads to weak northward advection of surface waters and ice and thus relatively weak AW upwelling (Fig. 9). Accordingly c4 is found deeper in the water column during summer when a positive summer AO also supports a strong inflow of LHW and surface waters from the KS (Janout et al. 2015) and in agreement with a strong occurrence of LHW type c2.

5. Summary and conclusions

Along its path from west to east along the Siberian continental slope Atlantic Water in the Arctic Ocean is found to be modified along the Barents Sea and Kara Sea continental margins. This modification is caused by shelf waters as identified by correlated changes in salinity and $\delta^{18}O$ properties that allow us to distinguish among river water, sea-ice meltwater and sea-ice related addition of brines. No additional salinity/$\delta^{18}O$ property changes are detectable within the core of the Atlantic Water further downstream along the Laptev Sea continental slope, within the Transpolar Drift and the EGC in western Fram Strait.

Inter annual differences in shelf water contributions are detected in a regional comparison. Evidence for a modification of Atlantic Water by brine released during sea-ice formation is found in 2006 along the Siberian continental slope of the Laptev Sea between Severnaya Zemlya and the New Siberian Islands (~110°E to ~145°E), while enhanced brine contributions were absent in all other sampled years. Therefore we suggest that sporadic Atlantic Water modification by sea-ice formation occurs north of Severnaya Zemlya (Ivanov and Golovin, 2007) and that this signal is transported rapidly along the Siberian continental margin.

Different types of Lower Halocline Water (LHW) identified by Principal Component Analysis show a consistent geographical distribution in all years. The saltiest LHW type is formed from modified Atlantic Water in the Barents and Kara Sea shelf areas. Our Principal

Component Analysis shows that further components of LHW are fed into the halocline in the north-western Laptev Sea supplied by waters from the south eastern Kara Sea.

LHW types can be linked to dynamical features of the Vilkitsky Strait Current (Janout et al., 2015) and the Arctic Shelf Break Branch (Aksenov et al., 2011). We find the same water mass components at the continental slope and further offslope within the basin. Thus the suggested offslope and onslope branches of LHW (e.g. Dmitrenko et al., 2006) are not confirmed and no dedicated offslope and onslope components of LHW are found. Nevertheless there is a "break" in temperature observed with slightly higher temperatures over the continental margin in the depth range of the LHW (Dmitrenko et al., 2011; Timokhov et al., 2015). However the underlying mechanism responsible for the observed "break" remains an open question (Timokhov et al., 2015).

No further modification of LHW is seen in the eastern Laptev Sea but our analyses suggest a bifurcation of LHW at this location possibly with a branch continuing along the continental margin and a second branch along the Lomonosov Ridge.

Inter annual variations in the boundary depth between halocline and Atlantic Waters are observed and these are found to be consistent with variations in the winter AO for the investigated period, 2005-2009. While it is clear that our observations are consistent with an oceanic response to regional atmospheric forcing, we refrain from claiming that our data may establish a general correlation to AO indexes as the evaluated time period between 2005 and 2009 is short.

Our analysis demonstrates that Principal Component Analysis may be successfully used to analyze multi-parameter oceanographic data and help to decrease the degrees of freedom. Analysis based on $\delta^{18}O$ and salinity data alone is not sufficient to infer different LHW types. Our PCA based cluster analysis based on $\delta^{18}O$, hydrological and hydrochemical data lead to an independent identification of four different LHW types with significant physical meaning that are found to feed into the halocline at different locations from the Barents Sea to the north-western Laptev Sea and that can be linked to dynamical features of the Vilkitsky Strait Current and the Arctic Shelf Break Branch.

6. Acknowledgements

We are grateful to all of our colleagues who made it possible to successfully conduct the extensive fieldwork program in the Arctic Ocean. Figures were generated using ODV [Schlitzer, 2001], and the GMT mapping tool [Wessel and Smith, 1998]. We like to thank our reviewers for constructive suggestions that helped to considerably improve the manuscript.

EC received funding from the Russian Foundation for Basic Research (Grant No. 14-01-31053) and from the German-Russian cooperation 'System Laptev Sea' funded by the BMBF under grant 03G0639D. DB acknowledges funds from the German Research Foundation grant BA 1689/2-2.

References:

Aagaard, K., Coachman, L. and Carmack, E.: On the halocline of the Arctic Ocean, Deep-Sea Research, 28, 529–545, 1981.

Abrahamsen, E. P., Meredith, M. P., Falkner, K. K., Torres-Valdes, S., Leng, M. J., Alkire, M. B., Bacon, S., Laxon, S., Polyakov, I., Ivanov, V. and Kirillov, S.: Tracer-derived freshwater budget of the Siberian Continental Shelf following the extreme Arctic summer of 2007, Geophys. Res. Lett, 36(L07602), doi:10.1029/2009GL037341, 2009.

Aksenov, Y., Ivanov, V. V., Nurser, A. J. G., Bacon, S., Polyakov, I. V., Coward, A. C., Naveira-Garabato, A. C. and Beszczynska-Moeller, A.: The Arctic Circumpolar Boundary Current, Journal of Geophysical Research: Oceans, 116(C9), C09017, doi:10.1029/2010JC006637, 2011.

Bauch, D., Schlosser, P. and Fairbanks, R. F.: Freshwater balance and the sources of deep and bottom waters in the Arctic Ocean inferred from the distribution of $H_2{}^{18}O$, Progress in Oceanography, 35, 53–80, 1995.

Bauch, D., Erlenkeuser, H., Stanovoy, V., Simstich, J. and Spielhagen, R. F.: Freshwater distribution and brine waters in the southern Kara Sea in summer 1999 as depicted by $\delta^{18}O$ results, in Siberian river run-off in the Kara Sea; characterisation, quantification, variability and environmental significance, Proceedings in Marine Science, edited by R. Stein, K. Fahl, D. Fuetterer, E. Galimov, and O. Stepanets, pp. 73–90, Elsevier, Amsterdam., 2003.

Bauch, D., Erlenkeuser, H. and Andersen, N.: Water mass processes on Arctic shelves as revealed from ^{18}O of H_2O, Global and Planetary Change, 48, 165–174, doi:10.1016/j.gloplacha.2004.12.011., 2005.

Bauch, D., J. Hölemann, S. Willmes, M. Gröger, A. Novikhin, A. Nikulina, H. Kassens and Timokhov, L.: Changes in distribution of brine waters on the Laptev Sea shelf in 2007, J. Geophys. Res., 115, C11008, doi:10.1029/2010JC006249, 2010.

Bauch, D., Gröger, M., Dmitrenko, I., Hölemann, J., Kirillov, S., Mackensen, A., Taldenkova, E. and Andersen, N.: Atmospheric controlled freshwater water release at the Laptev Sea Continental margin, Polar Res., 30, 5858, doi:10.3402/polar.v30i0.5858, 2011a.

Bauch, D., Rutgers van der Loeff, M., Andersen, N., Torres-Valdes, S., Bakker, K. and Abrahamsen, E. P.: Origin of freshwater and polynya water in the Arctic Ocean halocline in summer 2007, Progress in Oceanography, 91, 482–495, doi:10.1016/j.pocean.2011.07.017, 2011b.

Bauch, D., Torres-Valdes, S., Polyakov, I., Novikhin, A., Dmitrenko, I., McKay, J. and Mix, A.: Halocline water modification and along-slope advection at the Laptev Sea continental margin, Ocean Sci., 10(1), 141–154, doi:10.5194/os-10-141-2014, 2014.

Bekryaev, R. V., Polyakov, I. V. and Alexeev, V. A.: Role of Polar Amplification in Long-Term Surface Air Temperature Variations and Modern Arctic Warming, J. Climate, 23(14), 3888–3906, doi:10.1175/2010JCLI3297.1, 2010.

Dmitrenko, I. A., Polyakov, I. V., Kirillov, S. A., Timokhov, L. A., Simmons, H. L., Ivanov, V. V. and Walsh, D.: Seasonal variability of Atlantic water on the continental slope of the Laptev Sea during 2002–2004, Earth and Planetary Science Letters, 244(3–4), 735–743, doi:10.1016/j.epsl.2006.01.067, 2006.

Dmitrenko, I. A., Bauch, D., Kirillov, S. A., Koldunov, N., Minnett, P. J., Ivanov, V. V., Hölemann, J. A. and Timokhov, L. A.: Barents Sea upstream events impact the properties of Atlantic water inflow into the Arctic Ocean: Evidence from 2005-2006 downstream observations., Deep Sea Res. I, 56, 513–527, doi: 10.1016/j.dsr.2008.11.005, 2009.

Dmitrenko, I. A., Ivanov, V. V., Kirillov, S. A., Vinogradova, E. L., Torres-Valdes, S. and Bauch, D.: Properties of the Atlantic derived halocline waters over the Laptev Sea continental margin: Evidence from 2002 to 2009, Journal of Geophysical Research, 116(C10), C10024, doi:10.1029/2011JC007269, 2011.

Frank, M.: Spurenstoffuntersuchungen zur Zirkulation im Eurasischen Becken des Nordpolarmeeres, PhD thesis, Univ. Heidelberg, Germany, pp. 100, 1996.

Holland, M. M. and Bitz, C. M.: Polar amplification of climate change in coupled models, Climate Dynamics, 21(3-4), 221–232, doi:10.1007/s00382-003-0332-6, 2003.

Itkin, P., Losch, M. and Gerdes, R.: Landfast ice affects the stability of the Arctic halocline: Evidence from a numerical model, Journal of Geophysical Research C: Oceans, 120(4), 2622–2635, doi:10.1002/2014JC010353, 2015.

Ivanov, V. V. and Golovin, P. N.: Observations and modeling of dense water cascading from the northwestern Laptev Sea shelf, Journal of Geophysical Research: Oceans, 112(C9), C09003, doi:10.1029/2006JC003882, 2007.

Janout, M., Aksenov, Y., Hölemann, J., Rabe, B., Schauer, U., Polyakov, I., Bacon, S., Coward, A., Karcher, M. and Lenn, Y. D.: Kara Sea freshwater transport through Vilkitsky Strait: Variability, forcing, and further pathways toward the western Arctic Ocean from a model and observations, Journal of Geophysical Research: Oceans, 2015.

Mauldin, A., Schlosser, P., Newton, R., Smethie, W. M., Bayer, R., Rhein, M. and Jones, E. P.: The velocity and mixing time scale of the Arctic Ocean Boundary Current estimated with transient tracers, Journal of Geophysical Research: Oceans, 115(C8), 2010.

Newton, R., Schlosser, P., Martinson, D. G. and Maslowski, W.: Freshwater distribution in the Arctic Ocean: Simulation with a high resolution model and model-data comparison, J. Geophys. Res., 113(C05024), doi:10.1029/2007JC004111, 2008.

North, G., Bell, T., Cahalan, R. and Moeng, F.: Sampling errors in the estimation of empirical orthogonal functions, Monthly Weather Review, 10, 699–706, 1982.

Overland, J. E. and Wang, M.: Large-scale atmospheric circulation changes are associated with the recent loss of Arctic sea ice, Tellus A, 62(1), 1–9, doi:10.1111/j.1600-0870.2009.00421.x, 2010.

Overland, J. E. and Wang, M.: When will the summer arctic be nearly sea ice free?, Geophysical Research Letters, 40, 1–5, doi:10.1002/grl.50316, 2013.

Pnyushkov, A. V., Polyakov, I. V., Ivanov, V. V., Aksenov, Y., Coward, A. C., Janout, M. and Rabe, B.: Structure and variability of the boundary current in the Eurasian Basin of the Arctic Ocean, Deep Sea Research Part I: Oceanographic Research Papers, 101(0), 80–97, doi:10.1016/j.dsr.2015.03.001, 2015.

Rigor, I. G., Wallace, J. M. and Colony, R. L.: Response of sea ice to the Arctic Oscillation, Journal of Climate, 15(18), 2648–2663, 2002.

Rudels, B.: Atlantic sources of the Arctic Ocean surface and halocline waters, Polar Research, 23(2), 181–208, 2004.

Rudels, B., Anderson, L. G. and Jones, E. P.: Formation and evolution of the surface mixed layer and halocline of the Arctic Ocean, Journal of Geophysical Research: Oceans, 101(C4), 8807–8821, doi:10.1029/96JC00143, 1996.

Schauer, U.: The expedition ARKTIS-XXII/2 of the research vessel "Polarstern" in 2007, Alfred-Wegener Institute for Polar and Marine Research, Bremerhaven., 2008.

Schauer, U., Loeng, H., Rudels, B., Ozhigin, V. K. and Dieck, W.: Atlantic Water flow through the Barents and Kara Seas, Deep-Sea Research I, 49, 2281–2298, 2002.

Schlitzer, R.: Ocean Data View, http://www.awi-bremerhaven.de/GEO/ODV., 2001.

Schlosser, P., Bauch, D., Bönisch, G. and Fairbanks, R. F.: Arctic river-runoff: mean residence time on the shelves and in the halocline, Deep-Sea Research I, 41(7), 1053–1068, 1994.

Schmidt, G. A.: Global Seawater Oxygen-18 Database, http://data.giss.nasa.gov/o18data/, 1999.

Steele, M. and Boyd, T.: Retreat of the cold halocline layer in the Arctic Ocean, Journal of Geophysical Research, 103(C5), 10,419–10,435, 1998.

Timokhov, L., Ashik, I., Dmitrenko, I., Hoelemann, J., Kassens, H., Kirillov, S., Polyakov, I. and Sokolov, V.: Extreme changes of the Arctic Ocean during and after IPY 2007/2008, Polarforschung, 81(2), 85–102, 2012.

Timokhov, L., Hölemann, J., Ipatov, A., Janout, M. and Kassens, H.: Cold shelf waters of the Laptev Sea in the summer of 2013, Problems of Arctic and Antarctic, 104(2), 81–92, 2015.

Ward, J. H.: Hierarchical Grouping to Optimize an Objective Function, J. Am. Statist. Assoc., 58, 236–244, 1963.

Wessel, P. and Smith, W. H. F.: New improved version of the Generic Mapping Tools released, EOS Trans. AGU, 79, 579, 1998.

Woodgate, R. A., Aagaard, K., Muench, R. D., Gunn, J., Björk, G., Rudels, B., Roach, A. T. and Schauer, U.: The Arctic Ocean Boundary Current along the Eurasian slope and the adjacent Lomonosov Ridge: Water mass properties, transports and transformations from moored instruments, Deep-Sea Research I, 48, 1757–1792, 2001.

Highlights:

- Atlantic Water modified by sea-ice melt and meteoric water at Barents Sea slope
- LHW may be divided into different types by Principal Component Analysis (PCA)
- high salinity LHW-type forms in the Barents and Kara seas
- low salinity LHW-types form in the western Laptev Sea or enter via Vilkitsky Strait
- PCA does not support a distinction between onshore and offshore LHW branches